e-ISSN: 2805-5756

PENERBIT PRESS
UNIVERSITI TEKNOLOGI MARA

Available online at
https://jaeds.uitm.edu.my

Journal of Applied Engineering Design and Simulation 6(2) 2026, 14-26

Journal of Applied Engineering Design and Simulation

Simulation-driven evaluation and selection of analog rice extrusion die geometry using design of experiments and finite element analysis

Rosniza Rabilah[1], Noor Iswadi Ismail[1*], Puteri Nur Aisyah Megat Shaharuddin[1]

[1]Faculty of Mechanical Engineering, Universiti Teknologi MARA Cawangan Pulau Pinang, Permatang Pauh Campus, 13500 Permatang Pauh, Penang, Malaysia

ARTICLE INFO

Article history:
Received 02 July 2026
Revised 19 August 20206
Accepted 28 August 2026
Online first 25 September 2026
Published 25 September 2026

Keywords:
Extrusion die
Analog rice
Finite element analysis
Design optimization
Aluminum Alloy 6061

DOI:
10.24191/jaeds.v6i2.203

ABSTRACT

Analog rice extrusion dies must resist the applied extrusion load while maintaining low deformation, yet their structural geometry is rarely evaluated systematically before fabrication. This study aims to quantify the effects of edge fillet diameter and die-hole thickness on maximum von Mises stress and total deformation, and to identify the best-performing configuration within a predefined design space. Nine die configurations were generated using a 3^2 full factorial design with fillet diameters of 1, 2, and 3 mm and hole thicknesses of 10, 12, and 14 mm. Each configuration underwent one deterministic static finite element analysis in Altair SimLab under identical material properties, boundary conditions, mesh settings, and a 7117 N design load. The die material was Aluminum Alloy 6061-T6. Maximum stress ranged from 22.757 to 43.979 MPa, while deformation ranged from 0.008 to 0.016 mm. Across the evaluated levels, increasing both variables reduced the two structural responses, with hole thickness showing the larger main effect. Exploratory main-effects ANOVA and response models supported the observed trends, although inferential results were interpreted cautiously because the simulations were not independently replicated. The 3 mm fillet and 14 mm hole thickness configuration produced the lowest simulated stress and deformation among the nine cases. It is therefore reported as the best-performing tested configuration rather than a globally optimised design. The workflow supports pre-fabrication screening of analog rice extrusion dies and identifies priorities for subsequent experimental and thermo-mechanical validation.

[1*]Corresponding author. *E-mail address*: iswadi558@uitm.edu.my

Nomenclature (Greek symbols towards the end)

σ	Stress (MPa)
δ	Deformation (mm)

Abbreviations

DOE	Design of experiment
CAD	Computer-aided design
FEA	Finite element analysis
ANOVA	Analysis of variance
RSM	Response surface methodology
DF	Degree of freedom

1. INTRODUCTION

Rice remains a staple food for more than half of the global population, creating continued demand for products that support food security and dietary diversification [1]. Analog rice consists of rice-like grains produced from alternative carbohydrate sources. Studies have demonstrated analog rice based on sago, mung bean, corn, cassava, and banana flour [2-4]. Extrusion is widely used because mixing, conveying, and shaping can be integrated into a continuous process [5-6]. Reported screw speeds, barrel temperatures, and feed moisture contents vary substantially with formulation and product requirements [7-9]. These conditions influence material flow, starch transformation, and extrudate geometry. In addition to processing conditions, die geometry governs pressure transfer, stress concentration, deformation, and the dimensional stability of the outlet. Reviews of food extrusion and printing systems identify die geometry as an important design factor [10-12].

Most analog rice studies emphasize formulation, nutritional properties, extrusion conditions, and product characterization. The structural response of a rice-shaped extrusion die before fabrication has received less attention. Features such as section thickness, outlet geometry, and fillet transitions affect stress distribution and mechanical behaviour of extrusion systems [13-15]. The absence of a systematic pre-fabrication assessment makes it difficult to compare candidate geometries under controlled loading, which may increase reliance on trial-and-error prototyping.

A simulation-driven approach can screen candidate geometries before fabrication. Finite element analysis (FEA) estimates stress and deformation under prescribed material, loading, and boundary conditions, while a factorial design provides a structured comparison of geometric variables [16-19]. Nevertheless, evidence for analog rice die geometry remains limited, particularly for the combined effects of edge fillet diameter and die-hole thickness.

Accordingly, this study has two specific objectives: (1) to quantify the individual effects of edge fillet diameter and die-hole thickness on maximum von Mises stress and total deformation under a constant simulated extrusion load; and (2) to identify the best-performing configuration among nine predefined designs using an integrated CAD-DOE-FEA and response-modelling workflow. The study is limited to static structural simulation. It does not evaluate dough preparation, material flow, thermal effects, bulk density, expansion ratio, or the physical dimensions of extruded grains.

2. METHODOLOGY

2.1 Die Geometry and Design Variables

The extrusion die was designed with elliptical outlets based on measured Basmati rice dimensions and adapted for a small-scale pasta-type extrusion system. Three-dimensional models were developed in SolidWorks. Edge fillet diameter and die-hole thickness were selected as the only varying geometric factors because both can affect the load path and local stiffness around the outlets.

Fillet diameter was evaluated at 1, 2, and 3 mm, while die-hole thickness was evaluated at 10, 12, and 14 mm. The outer profile, overall dimensions, outlet size and arrangement, material, applied load, boundary conditions, element type, and mesh settings were held constant. Thus, differences among the nine simulation outputs arose from the two prescribed geometric factors within the assumptions of the model.

2.2 Full Factorial Design of Experiments

A 3^2 full factorial design was used to generate nine CAD and FEA configurations (Table 1). Each cell of the design matrix represented one unique combination of fillet diameter and hole thickness. One deterministic static FEA run was completed for each configuration. No independent physical extrusion experiments or repeated stochastic simulations were conducted. The nine runs therefore compared numerical design cases rather than experimental replicates. This distinction is considered when interpreting the exploratory ANOVA and response models.

Table 1. Full factorial DOE matrix for analog rice die configurations

Die	Fillet diameter, D (mm)	Hole thickness, T (mm)	Description
1	1	10	small fillet, thin wall
2	1	12	small fillet, medium wall
3	1	14	small fillet, thick wall
4	2	10	medium fillet, thin wall
5	2	12	medium fillet, medium wall
6	2	14	medium fillet, thick wall
7	3	10	large fillet, thin wall
8	3	12	large fillet, medium wall
9	3	14	large fillet, thick wall

2.3 Material Properties and Finite Element Setup

Aluminum Alloy 6061-T6 was represented as a homogeneous, isotropic, linear-elastic solid with a density of 2700 kg/m³, Young's modulus of 69 GPa, and Poisson's ratio of 0.33 (Table 2). This assumption was considered appropriate because all predicted stresses were below the material yield strength [20]. Static analyses were conducted in Altair SimLab. The outer mounting surfaces were fixed and a total design load of 7117 N was distributed over the internal die-hole region. Second-order Tet10 elements were used to represent curved fillet and outlet boundaries. Identical material properties, load application, constraints, element formulation, and mesh settings were used for all nine models. The study did not simulate dough flow or temperature-dependent behaviour; therefore, no dough was prepared and no pre-extrusion dough test was performed.

Table 2. Material properties used for FEA simulation

Property	Value
Density	2.7 g/cm3
Young's modulus	69 GPa
Poisson's ratio	0.33
Material model	Linear elastic

2.4 Exploratory Statistical and Response Analysis

Main effects were summarized from the nine FEA outputs. Because there was one deterministic result per factorial cell, a conventional replicated two-factor ANOVA with a separate estimable interaction and pure error was not possible. An additive two-factor ANOVA was used as an exploratory screening analysis; the four residual degrees of freedom contain any unmodelled interaction and numerical/model discrepancy. Accordingly, F- and p-values are reported as conditional indicators and not as confirmatory experimental inference. Linear and second-order response models were also fitted by least squares to describe trends within the tested range. Model fit was compared using R^2, while preference was given to the simpler model when additional terms provided negligible improvement. Response surfaces were used to locate the lowest predicted responses only within the evaluated factor bounds. Figure 1 summarizes the workflow, and Figure 2 presents the die geometry used in CAD modelling and FEA.

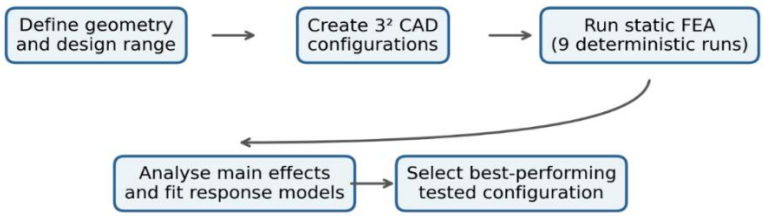


Fig. 1. Simulation-driven workflow used to evaluate and select the die configuration

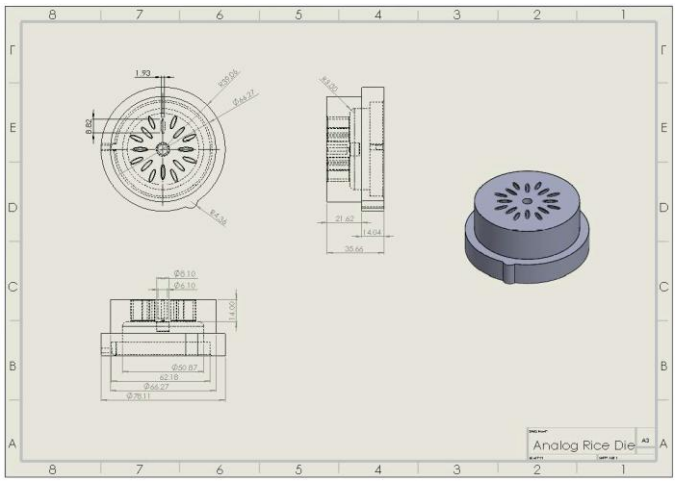


Fig. 2. CAD model and engineering drawing of the analog rice extrusion die

3. RESULTS AND DISCUSSION

3.1 Finite Element Results

The nine deterministic FEA runs produced maximum von Mises stresses from 22.757 to 43.979 MPa and maximum deformations from 0.008 to 0.016 mm (Table 3). Representative contours for Dies 1, 5, and 9 are shown in Figure 3. Within the tested combinations, both responses generally decreased as fillet diameter and hole thickness increased. Die 9 (3 mm fillet; 14 mm hole thickness) recorded the lowest stress and deformation, whereas Die 1 recorded the highest values. Relative to Die 1, Die 9 reduced simulated stress by 48.25% and deformation by 50.00%. These values describe the tested numerical cases and do not constitute replicated experimental measurements.

The trend is mechanically consistent with a smoother fillet transition reducing local stress concentration and a thicker section increasing bending stiffness. Nevertheless, this explanation remains a simulation-based interpretation because thickness was not isolated in replicated physical extrusion tests. The result should therefore be validated experimentally under measured pressure and temperature histories before being generalized to manufacturing performance [16-18,22].

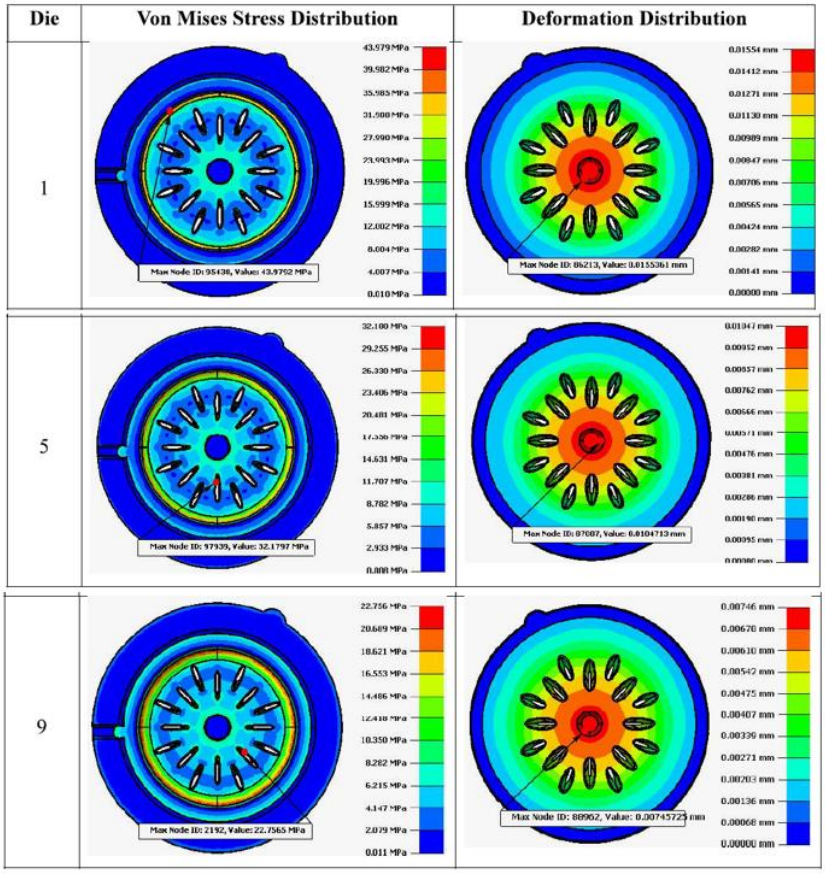


Fig. 3. Comparison of von Mises stress and deformation distributions for die 1, 5, and 9 configurations

Table 3. FEA results for maximum von Mises stress and total deformation

Die	Max von Mises stress (MPa)	Max deformation (mm)
1	43.979	0.016
2	38.139	0.011
3	33.091	0.009
4	41.435	0.014
5	32.180	0.011
6	26.308	0.008
7	37.769	0.013
8	30.985	0.010
9	22.757	0.008

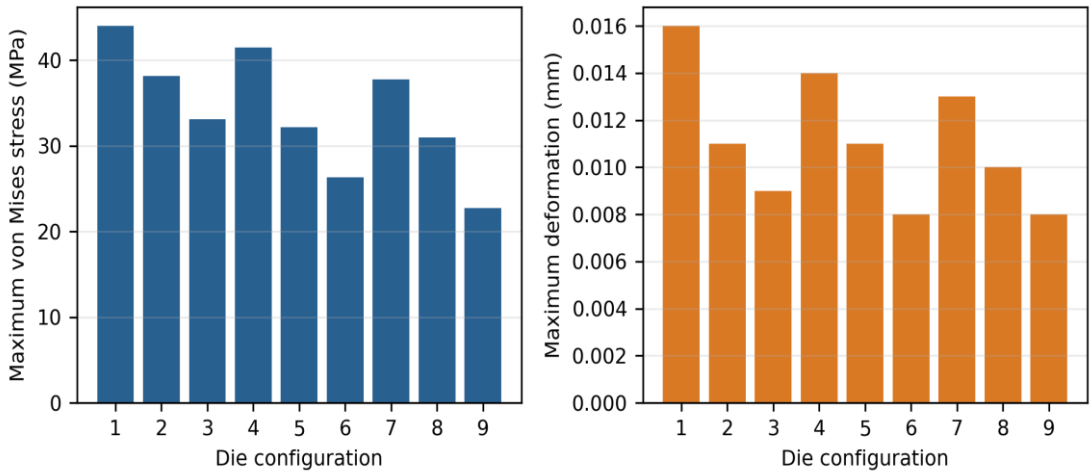


Fig. 4. Maximum von Mises stress and deformation for the nine deterministic FEA configurations

3.2 Effect of Fillet Diameter and Hole Thickness

Figure 5 presents the stress main effects averaged across the other factor. Increasing fillet diameter from 1 to 3 mm reduced mean maximum stress from 38.403 to 30.504 MPa. Increasing hole thickness from 10 to 14 mm produced a larger reduction, from 41.061 to 27.385 MPa. These comparisons are descriptive averages of the nine deterministic simulations.

For deformation (Figure 6), the mean decreased from 0.012 to 0.010 mm across the fillet levels and from 0.014 to 0.008 mm across the thickness levels. The larger thickness effect is consistent with increased section stiffness under the prescribed static load. Since no physical replication, pressure measurement, or thermo-mechanical test was performed, the proposed mechanism was not claimed as experimental proof.

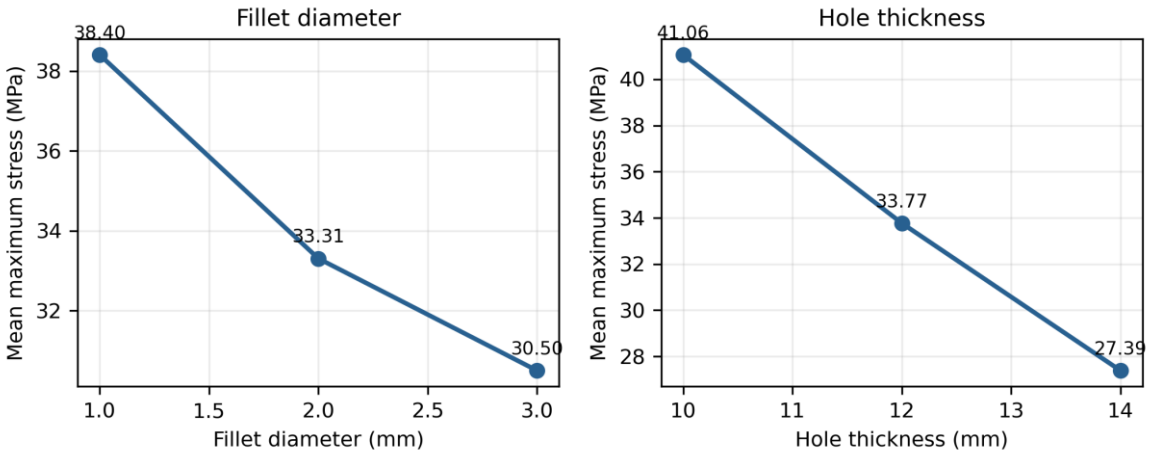


Fig. 5. Main effects of fillet diameter and hole thickness on maximum von Mises stress

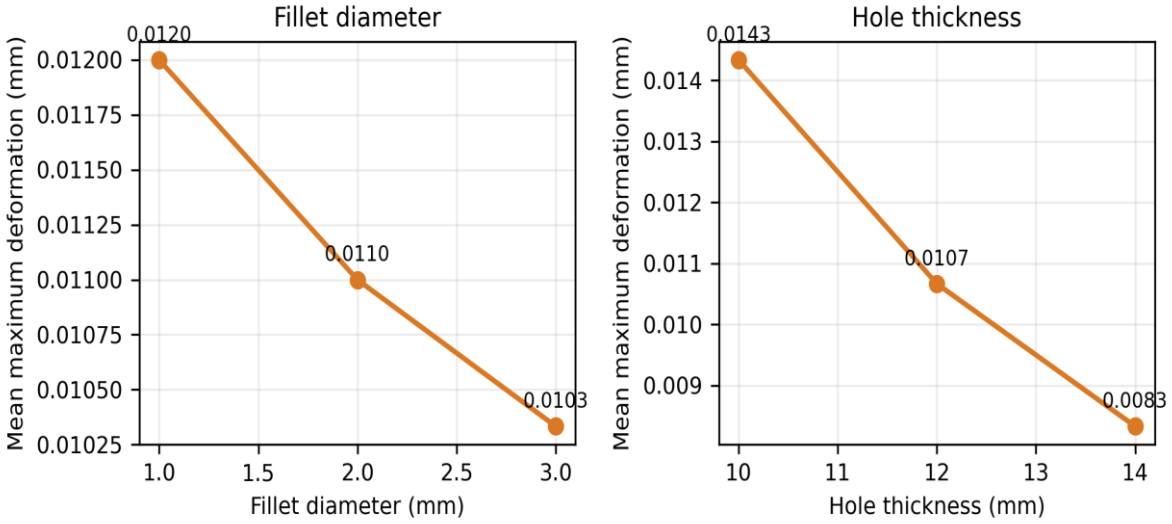


Fig. 6. Main effects of fillet diameter and hole thickness on maximum deformation

3.3 Exploratory ANOVA and Model Adequacy

Tables 4 and 5 present the additive main-effects ANOVA used for exploratory screening. Under this model, hole thickness produced the larger F-value for stress (72.24 versus 24.74) and deformation (301.91 versus 25.55). The corresponding conditional p-values were below 0.05. However, these values must be interpreted cautiously: with one result per design cell, the residual term also contains any interaction between the factors, and pure experimental error cannot be estimated. The analysis therefore ranks factor influence within the numerical design matrix rather than demonstrating repeatable physical significance.

Table 6 compares descriptive R^2 values for the fitted response models. The linear model gave R^2 = 0.9338 for stress, whereas the second-order model gave R^2 = 0.9693 for deformation. The cubic specification did not materially improve the deformation fit and was not selected. R^2 is used here as an in-

sample measure of agreement; predictive validation requires additional configurations or independent physical tests.

Figure 7 compares the exploratory F-values and shows that hole thickness had the larger main effect for both numerical responses. This ranking is restricted to the selected levels, loading assumptions, and static structural model.

Table 4. ANOVA summary for maximum von Mises stress

Source	DF	Sum of squares	Mean square	F-value	p-value
Fillet diameter	2	98.233	49.117	24.744	0.00559
Hole thickness	2	286.982	143.491	72.243	0.000726
Error	4	7.780	1.945	-	-
Total	8	392.995	-	-	-

Table 5. ANOVA summary for maximum deformation

Source	DF	Sum of squares	Mean square	F-value	p-value
Fillet diameter	2	3.49E-05	1.74E-05	25.546	0.00527
Hole thickness	2	5.87E-05	2.94E-05	301.907	4.33E-05
Error	4	3.88E-07	9.73E-08	-	-
Total	8	1.41E-04	-	-	-

Table 6. Comparison of regression fit quality using R2 values

Fit specification	Stress R2	Deformation R2
Linear	0.9338129	0.9490483
Squared	0.8977159	0.9692672
Cubic	0.8977159	0.9692972

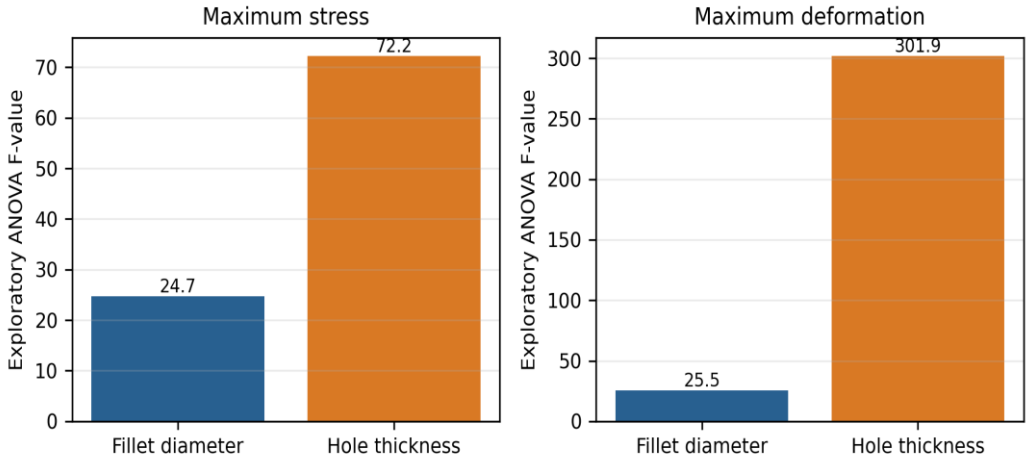


Fig. 7. Exploratory ANOVA F-values for the two geometric factors

3.4 Response Models and Design-Space Evaluation

The fitted second-order equations used to describe the structural responses within the tested factor bounds are:

For maximum von Mises stress:

$$\sigma = 102.899 - 8.532D - 6.150T + 1.146D2 + 0.114T2 \quad \text{(MPa)} \quad (1)$$

For total deformation:

$$\delta = 0.05603 - 0.0009958D - 0.005724T + 0.00002148D2 + 0.0001739T2 \quad \text{(mm)} \quad (2)$$

where D is fillet diameter in mm and T is die hole thickness in mm.

Figures 8 and 9 show the fitted response surfaces. Both surfaces decline toward the upper tested levels of fillet diameter and hole thickness. The lowest predicted responses within the defined 1-3 mm and 10-14 mm design space occurred at 3 mm and 14 mm, consistent with the direct FEA result for Die 9.

The agreement between the fitted surfaces and the simulated design cases supports the use of the models for interpolation within the tested range. It does not establish a global optimum outside that range. The selected geometry should also not be extrapolated to other materials, outlet arrangements, loads, or temperatures without new analyses and experimental validation.

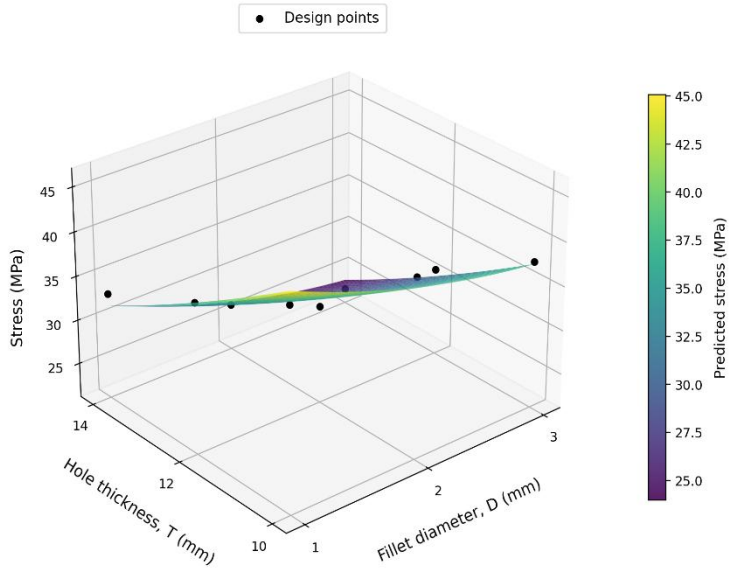


Fig. 8. Fitted response surface for maximum von Mises stress within the tested design space

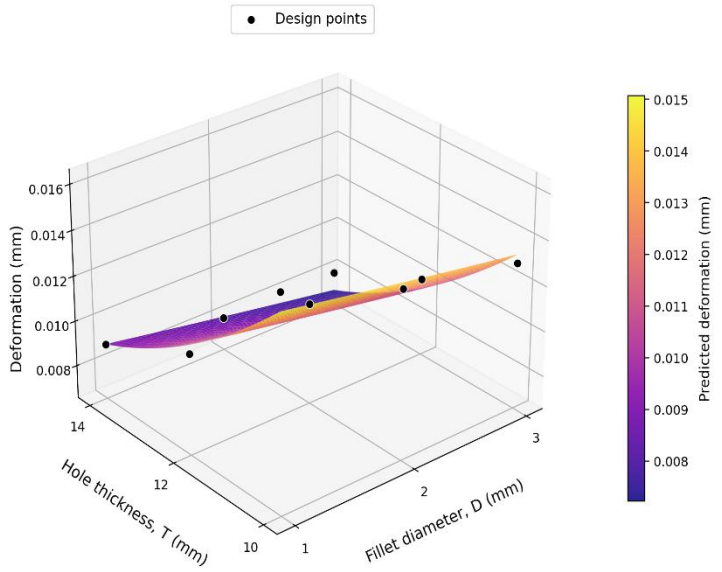


Fig. 9. Fitted response surface for maximum deformation within the tested design space

3.5 Best-Performing Tested Configuration

Die 9, with a 3 mm fillet diameter and 14 mm hole thickness, produced the lowest simulated stress (22.757 MPa) and deformation (0.008 mm) among the nine evaluated configurations (Table 7). It is therefore identified as the best-performing tested configuration, not as a globally optimised die. The predicted stress was below the yield strength of Aluminum Alloy 6061-T6 under the specified static load. This finding supports fabrication and experimental validation of Die 9 as the next development step. Its performance under real dough flow, measured pressure, thermal loading, cyclic operation, wear, and dimensional-quality requirements remains to be established.

Table 7. Best-performing configuration within the tested design space

Parameter	Selected value
Fillet diameter	3 mm
Die hole thickness	14 mm
Maximum von Mises stress	22.757 MPa
Maximum deformation	0.008 mm
Stress reduction relative to Die 1	48.25%
Deformation reduction relative to Die 1	50.00%

4. CONCLUSIONS

This study met its first objective by quantifying the effects of edge fillet diameter and die-hole thickness across nine static FEA configurations. Maximum von Mises stress ranged from 22.757 to 43.979 MPa and maximum deformation from 0.008 to 0.016 mm. Hole thickness showed the larger descriptive main effect for both responses within the tested range. The second objective was met by identifying Die 9 (3 mm fillet and 14 mm hole thickness) as the best-performing tested configuration, with 48.25% lower stress and

50.00% lower deformation than Die 1. Because each factorial cell contains one deterministic simulation, the ANOVA is exploratory and cannot estimate pure experimental error or independently separate interaction. The result is therefore a design-screening outcome rather than evidence of a global optimum or validated production performance. Future work should fabricate the selected configuration, conduct replicated extrusion trials, measure the actual pressure and temperature histories, assess mesh and model sensitivity, and evaluate material flow, bulk density, expansion ratio, and grain dimensional accuracy using fully specified test procedures.

5. ACKNOWLEDGEMENTS/FUNDING

The authors would like to acknowledge Universiti Teknologi MARA for providing technical facilities and academic support for this research. The authors also gratefully acknowledge the financial support provided by Ladang Konjak Sdn. Bhd. under Grant No. 100-TNPCI/PRI 16/6/2 (085/2024).

6. AUTHORS' CONTRIBUTIONS

Rosniza Rabilah: Conceptualisation, methodology and writing-original draft;

Noor Iswadi Ismail: Supervision, validation, and writing-review and editing;

Puteri Nur Aisyah Megat Shaharuddin: Formal analysis, investigation, and visualisation.

7. CONFLICT OF INTEREST STATEMENT

The authors declare no competing financial or personal interests that could have influenced the work reported in this paper.

8. DECLARATION OF GENERATIVE AI IN THE WRITING PROCESS

During the preparation of this work, the authors used ChatGPT for language editing and formatting assistance. After using this tool, the authors reviewed and edited the content as needed and take full responsibility for the content of the published article.

9. DATA AVAILABILITY/SUPPLEMENTARY MATERIALS

All data generated or analysed during this study are included in this published article.

10. ETHICS STATEMENT

The authors declare that this research did not involve human or animal subjects.

11. REFERENCES

[1] W. Leonard, P. Zhang, D. Ying, and Z. Fang, "Application of extrusion technology in plant food processing byproducts: An overview," *Comprehensive Reviews in Food Science and Food Safety*, vol. 19, no. 1, pp. 218-246, 2020, doi: 10.1111/1541-4337.12514.

[2] S. Sumardiono, I. Pudjihastuti, E. Supriyo, H. Kusumayanti, and A. N. Prastika, "Production and physicochemical characterization of analog rice obtained from sago flour, mung bean flour, and corn flour using hot extrusion technology," *Foods*, vol. 10, no. 12, Art. no. 3023, 2021, doi: 10.3390/foods10123023.

[3] M. Mahendradatta, E. Assa, J. Langkong, A. B. Tawali, and D. G. Nadhifa, "Development of analog rice made from cassava and banana with the addition of katuk leaf (Sauropus androgynous L. Merr.) and soy lecithin for lactating women," *Foods*, vol. 13, no. 10, Art. no. 1438, 2024, doi: 10.3390/foods13101438.

[4] V. P. R. Septiani *et al*., "Development of sago-based analog rice using Kansei and value engineering," *Pertanika Journal of Science and Technology*, vol. 31, no. 6, pp. 2947-2960, 2023, doi: 10.47836/pjst.31.6.17.

[5] L. Nateghi, A. S. Gohari, M. N. Tabar, and M. Alipour, "Analog rice: Processing and nutrition value," *Journal of Human, Health and Halal Metrics*, vol. 2, no. 2, pp. 18-24, 2021, doi: 10.30502/jhhhm.2021.300053.1038.

[6] D. G. Nadhifa *et al*., "Characterization of analog rice produced from various carbohydrate sources and their functional components: A review," *Discover Food*, 2025, doi: 10.1007/s44187-025-00473-9.

[7] Z. A. S. Bahlawan, A. C. Kumoro, Megawati, and S. K. Wahono, "Physico-chemical characteristics of novel analog rice from fermented sorghum flour by Rhizopus oligosporus and soybean flour," *Current Research in Nutrition and Food Science*, vol. 11, no. 3, p. 1022, 2023, doi: 10.12944/CRNFSJ.11.3.09.

[8] Y. S. Darmanto *et al*., "Characteristic of analog rice made from arrowroot (Maranta arundinacea) and seaweed (Gracilaria verrucosa) flour fortified with fish collagen," *Food Research*, vol. 6, no. 5, 2022, doi: 10.26656/fr.2017.6(5).473.

[9] S. Choton, N. Gupta, J. D. Bandral, N. Anjum, and A. Choudary, "Extrusion technology and its application in food processing: A review," *The Pharma Innovation Journal*, vol. 9, no. 2, pp. 162-168, 2020.

[10] V. Raja, S. Nimbkar, J. A. Moses, S. V. R. Nair, and C. Anandharamakrishnan, "Modeling and simulation of 3D food printing systems: Scope, advances, and challenges," *Foods*, vol. 12, no. 18, Art. no. 3412, 2023, doi: 10.3390/foods12183412.

[11] T. M. Oyinloye and W. B. Yoon, "Application of computational fluid dynamics (CFD) simulation for the effective design of food 3D printing (a review)," *Processes*, vol. 9, no. 11, Art. no. 1867, 2021, doi: 10.3390/pr9111867.

[12] H. Zhou, Q. Wang, and J. Zhang, "Extruder die innovations for the texturization of plant proteins applied in plant-based products," *Comprehensive Reviews in Food Science and Food Safety*, vol. 25, no. 1, Art. no. e70367, 2026, doi: 10.1111/1541-4337.70367.

[13] A. Szpicer, W. Binkowska, I. Wojtasik-Kalinowska, S. M. S. Zebari, and A. Poltorak, "Application of computational fluid dynamics simulations in food industry," *European Food Research and Technology*, vol. 249, pp. 1411-1430, 2023, doi: 10.1007/s00217-023-04231-y.

[14] A. Razeghiyadaki, D. Zhang, D. Wei, and A. Perveen, "Optimization of polymer extrusion die based on response surface method," *Processes*, vol. 8, no. 9, Art. no. 1043, 2020, doi: 10.3390/pr8091043.

[15] M. Alghamdy *et al*., "Enhancing printability through design feature analysis for 3D food printing," *Applied Sciences*, vol. 14, no. 20, Art. no. 9587, 2024, doi: 10.3390/app14209587.

[16] C. Fricke, D. Wolff, M. Kemmerling, and S. Elgeti, "Investigation of reinforcement learning for shape optimization of profile extrusion dies," *Advances in Computational Science and Engineering*, vol. 1, no. 1, pp. 1-35, 2023, doi: 10.3934/acse.2023001.

[17] J. P. O. Vidal *et al*., "Enhancing extrusion die design efficiency through high-performance computing," *Mechanics of Time-Dependent Materials*, 2025, doi: 10.1007/s11012-024-01919-7.
[18] A. Gaspar-Cunha et al., "Optimization of polymer processing: A review (part I: extrusion)," *Polymers*, vol. 14, no. 2, Art. no. 384, 2022, doi: 10.3390/polym14020384.
[19] M. A. Hadiyat, "Response surface methodology using observational data: A systematic literature review," *Applied Sciences*, vol. 12, no. 20, Art. no. 10663, 2022, doi: 10.3390/app122010663.
[20] E. A. Abbas and K. K. Mansor, "Numerical and experimental investigation of the effect of strength of aluminum 6061 alloy on thickness reduction in single-point incremental forming," *Advances in Science and Technology Research Journal*, vol. 17, no. 4, pp. 271-281, 2023, doi: 10.12913/22998624/170713.
[21] R. R. Yadav, Y. Dewang, J. Raghuwanshi, and V. Sharma, "Finite element analysis of extrusion process using aluminum alloy," *Materials Today: Proceedings*, vol. 24, pp. 500-509, 2020, doi: 10.1016/j.matpr.2020.04.302.
[22] D. J. Leech, S. Lightfoot, and T. Jorgensen, "Geometric pressure minimisation of a theoretical die for ceramic extrusion," arXiv:2007.12588, 2020, doi: 10.48550/arXiv.2007.12588.



© 2026 by the authors. Submitted for possible open access publication under the terms and conditions of the Creative Commons Attribution (CC BY-NC-ND) license (http://creativecommons.org/licenses/by/4.0/).